Spectrum Management for Multi-Access Edge Computing in Autonomous Vehicular Networks

Haixia Peng, *Student Member, IEEE*, Qiang Ye, *Member, IEEE*, and Xuemin Shen, *Fellow, IEEE*

***Abstract*— In this paper, a dynamic spectrum management framework is proposed to improve spectrum resource utilization in a multi-access edge computing (MEC) in autonomous vehicular network (AVNET). To support the increasing communication data traffic and guarantee quality-of-service (QoS), spectrum slicing, spectrum allocating, and transmit power controlling are jointly considered. Accordingly, three non-convex network utility maximization problems are formulated to slice spectrum among base stations (BSs), allocate spectrum among autonomous vehicles (AVs) associated with a BS, and control transmit powers of BSs, respectively. Through linear programming relaxation and first-order Taylor series approximation, these problems are transformed into tractable forms and then are jointly solved through an alternate concave search (ACS) algorithm. As a result, the optimal spectrum slicing ratios among BSs, optimal BS-vehicle association patterns, optimal fractions of spectrum resources allocated to AVs, and optimal transmit powers of BSs are obtained. Based on our simulation, a high aggregate network utility is achieved by the proposed spectrum management scheme compared with two existing schemes.**

***Index Terms*— Multi-access edge computing, NFV, spectrum resource allocation, QoS-guaranteed service, autonomous vehicles.**

I. Introduction

RECENT advances in automobiles and artificial intelligence technology are promoting the developing of autonomous vehicles (AVs), which are becoming a reality [1] and are expected to be commercialized and appear on the roads in the coming years [2]. However, salient challenges in computing and communication remain to be addressed to support AV applications. From the computing perspective, various computing tasks need to be carried out on board for real-time environment sensing and driving decision making [3]. Moreover, enabling cooperative driving among AVs, such as platoon-based driving [4]–[7] and convoy-based driving [3], [8], also requires extra computing tasks. From the communication perspective, the vehicular network enables inter-AV information exchanging and provides high definition (HD) maps [9] to AVs to support vehicular safety and non-safety related applications [10], [11]. For example, cooperative driving requires inter-AV communications for sharing position, velocity, acceleration, and other cruise control information [5], [12]. All these required information exchanges among AVs increase the communication data traffic and are with differential quality-of-service (QoS) requirements.

Some achievements have been made to overcome the challenges in computing and communication in vehicular networks. Edge computing has been regarded as an effective technology to enhance computing and storing capabilities in vehicular networks while alleviating traffic load to the core network [13]–[15]. Via moving computing and storing resources to servers placed at the edge of the core network, vehicles can offload its computing tasks to edge servers. Another potential method to address the computing issue is enabling collaborative computing among vehicles [3], [16], [17]. In the scenarios with light computing task load, the on-board computing resource utilization can be improved through offloading computing tasks to the adjacent vehicles with idle computing power [3]. To address the communication issues in vehicular networks, interworking of multiple wireless access technologies has been widely accepted, such as the interworking of cellular network and dedicated short-range communications (DSRC) technologies [18]. To simultaneously address both computing and communication issues in vehicular networks, multi-access edge computing (MEC)[1] has recently been considered in some existing works [19], [20].

Inspired by existing works, a new architecture combines MEC with network function virtualization (NFV) and software defined networking (SDN) to address the challenges in computing and communication in autonomous vehicular networks (AVNETs) [21]. Via the MEC technology, 1) AVs with limited on-board computing/storing resources can offload the tasks requiring high computing/storing requirements to the MEC servers, such that a shorter response delay can be guaranteed through avoiding the data transfer between the core network and MEC servers; 2) multiple types of access technologies are permitted, thus moving AVs can access MEC servers via different base stations (BSs), such as Wi-Fi access points (Wi-Fi APs), road-side units (RSUs) [22], White-Fi infostations, and evolved NodeBs (eNBs). Moreover, by integrating SDN and NFV concepts in each MEC server [23]–[25], global network control is enabled, and therefore, the computing/storing resources placed at MEC servers can be dynamically managed

Manuscript received December 10, 2018; revised March 20, 2019; accepted May 17, 2019. Date of publication June 27, 2019; date of current version June 29, 2020. This work was supported by research grants from the National Natural Science Foundation of China (NSFC) under Grant 91638204 and from the Natural Sciences and Engineering Research Council (NSERC) of Canada. The Associate Editor for this paper was X. Cheng. *(Corresponding author: Qiang Ye.)*

The authors are with the Department of Electrical and Computer Engineering, University of Waterloo, Waterloo, ON N2L 3G1, Canada (e-mail: h27peng@uwaterloo.ca; q6ye@uwaterloo.ca; sshen@uwaterloo.ca).

Digital Object Identifier 10.1109/TITS.2019.2922656

[1] In 2017, mobile edge computing has been renamed to multi-access edge computing by the European Telecommunication Standards Institute (ETSI) to better reflect the growing interest and requirements in edge computing from non-cellular operators.

and various radio spectrum resources can be abstracted and sliced to the BSs and then be allocated to AVs by each BS.

Efficient management for computing, storing, and spectrum resources is of paramount importance for the MEC-based AVNET. However, it is challenging to simultaneously manage the three types of resources while guaranteeing the QoS requirements for different AV applications, especially in the scenario with a high AV density. In this paper, we focus on spectrum resource management which can be extended to multiple resource allocation as our future work. The main contributions of this work are summarized as follows:

1) By considering the tradeoff between spectrum resource utilization and inter-cell interference, we develop a dynamic two-tier spectrum management framework for the MEC-based AVNET, which can be easily extended to other heterogeneous networks.
2) Leveraging logarithmic and linear utility functions, we formulate three aggregate network utility maximization problems to fairly slice spectrum resources among BSs connected to the same MEC server, optimize BS-vehicle association patterns and resource allocation, and control the transmit power of BS.
3) Linear programming relaxation and first-order Taylor series approximation are used and an alternate concave search (ACS) algorithm is designed to jointly solve the three formulated optimization problems.

The remainder of this paper is organized as follows. First, the MEC-based AVNET is introduced in Section II, followed by the dynamic spectrum management framework and the communication model. In Section III, three optimization problems are formulated to slice and allocate spectrum resources among BSs and among AVs and control the transmit power of BS. Then, the three problems are transformed to tractable problems and are jointly solved in Section IV. In Section V, extensive simulation results are presented to demonstrate the performance of the proposed spectrum management framework. Finally, we draw concluding remarks in Section VI.

II. System Model

In this section, we first present an MEC-based AVNET architecture and a dynamic spectrum management framework, and then describe the communication model under the considered AVNET.

A. MEC-Based AVNET Architecture

Based on a reference model suggested by the MEC ETSI industry specification group [19], we consider an MEC-based AVNET with one MEC server to support AV applications,[2] as shown in Fig. 1. The MEC server allows AVs to access the edge computing/storing resources through different wireless access technologies.

To improve the cost efficiency of MEC server placement and provide short response delays to the AVs, the MEC server should be placed close to the edge of the core network but not directly at each BS [21]. The communication hops between an MEC server and an AV is assumed to be two. Thus, a large number of AVs within the coverages of several neighboring BSs can be served by the same MEC server and the enlarged service area of the MEC server can better overcome the challenges caused by high AV mobility. The total coverages of BSs connected to an MEC server is defined as the service area of this server. To realize the resource virtualization process, including computing, storing, and spectrum resources, we consider a virtual wireless network controller at the MEC server. Through collecting information from the BSs and the AVs in the service area, resource management functions can run at the controller to adjust the virtual computing and storing resources to different AV tasks and to coordinate wireless access over the wide range of spectrum resources for AVs.

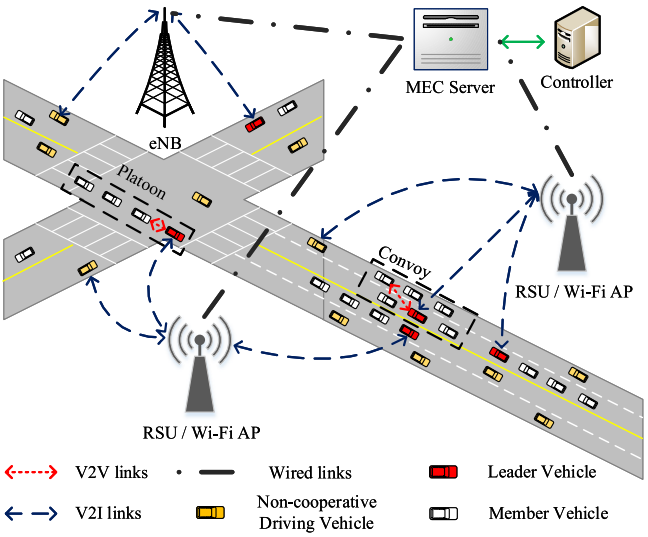

Fig. 1. An MEC-based AVNET model.

B. Dynamic Spectrum Management Framework

Due to the high AV mobility and heterogeneous AV applications, AVNET topology and QoS requirements change frequently, and therefore, resource allocation should be adjusted accordingly. To improve spectrum resource utilization, a dynamic spectrum management framework is developed for downlink transmission. Taking a one-way straight road with two lanes as an example in Fig. 2, two wireless access technologies, cellular and Wi-Fi/DSRC [26]–[29], are available to the AVs. Wi-Fi APs/RSUs and eNBs are uniformly deployed on one side of the road, where the ith Wi-Fi AP and the jth eNB are denoted by W_i and S_j, respectively. The transmit power of each eNB, P, is fixed and high enough to guarantee a wide-area coverage, such that all AVs can receive sufficient strong control signal or information signal from eNBs. Denote P_i' as the transmit power of Wi-Fi AP W_i, which is lower than P and is dynamically adjusted by the controller. For AVs within the overlapping area of two BSs, only one of the BSs is associated for downlink transmission.

[2]We take cooperative driving (platooning or convoying) as an AV application example, and AVs are grouped into cooperative driving vehicles (leader vehicles or member vehicles) and non-cooperative driving vehicles.

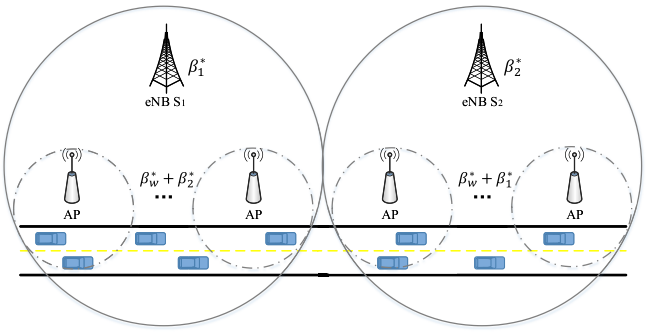

Fig. 2. A dynamic spectrum management framework.

We divide the eNBs into two groups, denoted by $\mathcal{B}_1$ and $\mathcal{B}_2$, where eNBs in the same group share the same spectrum resources and are not neighbored to each other. ENBs S_1 and S_2 shown in Fig. 2 are the two target eNBs from the two different sets, where $S_1 \in \mathcal{B}_1$ is adjacent to $S_2 \in \mathcal{B}_2$. Set of Wi-Fi APs under the coverage of eNB S_j is denoted by $\mathcal{A}_j$. Denote the total available spectrum resources for AV applications to be $R^{\max}$. After collecting the application requests from AVs via BSs, the controller performs dynamic spectrum management for downlink transmission. The procedure can be divided into two tiers as the following.

1) *Spectrum slicing among BSs:* The controller slices the spectrum resource, $R^{\max}$, into three slices with ratio set $\{\beta_1, \beta_2, \beta_w\}$ with $\beta_1 + \beta_2 + \beta_w = 1$, and allocates them to eNBs in $\mathcal{B}_1$, eNBs in $\mathcal{B}_2$, and Wi-Fi APs, respectively.
2) *Spectrum allocating among AVs:* Once the spectrum is sliced, each BS allocates its available spectrum resources to AVs associated to it. By allocating an appropriate amount of spectrum resources to each AV, the QoS requirements of various AV applications can be satisfied and the sum of transmission rates over the whole AVNET can be maximized.

Spectrum slicing among BSs, spectrum allocating among AVs, and transmit power controlling for Wi-Fi APs are updated once the traffic load of each eNB fluctuates, which is in a large time scale compared to network dynamic due to AV mobility. The traffic load of an eNB is defined as the average arrival traffic for AVs in the coverage of the eNB.

C. Communication Model

Assume the three slices of spectrum resources are mutually orthogonal, therefore, there is no inter-slice interference. To improve the spectrum resource utilization, two levels of spectrum reusing are considered. The first level is reusing the spectrum resource $\beta_w R^{\max}$ among all the Wi-Fi APs as long as with an acceptable inter-cell interference. Moreover, we assume that the Wi-Fi APs with no overlapping coverage area with an eNB can reuse the spectrum allocated to that eNB. Thus, the interference to eNBs caused by the Wi-Fi APs can be controlled by adjusting the transmit powers of the Wi-Fi APs while the spectrum resource utilization can be further improved by allowing each Wi-Fi AP to reuse either the spectrum resource $(\beta_w + \beta_1)R^{\max}$ or $(\beta_w + \beta_2)R^{\max}$.

According to the dynamic spectrum management framework presented in Section II-B, all the eNBs in $\mathcal{B}_1$ reuse the spectrum resource $\beta_1\ R^{\max}$ for downlink transmission. Denote $\mathcal{M}_j/M_j$ as the set/number of AVs within the coverage of eNB S_j. Then AV k, under the coverage of eNB S_1 (i.e., $k \in \mathcal{M}_1$), experiences two kinds of interference to the corresponding downlink: from transmissions of other eNBs in $\mathcal{B}_1$ and of Wi-Fi APs in the coverage of eNBs in $\mathcal{B}_2$. Thus, the spectrum efficiency at AV k ($k \in \mathcal{M}_1$) from eNB S_1 can be given by

$$r_1^k = \log_2\Big(1 + \frac{P_1\ G_1^k}{\sum\limits_{S_j \in \mathcal{B}_1, j \neq 1} P_j G_j^k + \sum\limits_{S_j \in \mathcal{B}_2} \sum\limits_{W_i \in \mathcal{A}_j} P_i' G_i'^k + \sigma^2}\Big), \tag{1}$$

where G_j^k ($G_i'^k$) is the channel power gain between eNB S_j (Wi-Fi AP W_i) and AV k, and σ^2 is the power spectrum density of the additive white Gaussian noise (AWGN). Similarly, the spectrum efficiency at AV k ($k \in \mathcal{M}_2$) from eNB S_2, r_2^k, can be obtained. Let R_j^k be the amount of spectrum allocated for AV k from eNB S_j. Then, the achievable transmission rates of AV k associated with eNBs S_1 (or S_2) can be expressed as

$$\gamma_1^k = R_1^k r_1^k \quad (\text{or } \gamma_2^k = R_2^k r_2^k). \tag{2}$$

Denote $\mathcal{N}_i/N_i$ as the set/number of AVs within the coverage of Wi-Fi AP W_i. Let $R_{2,g}'^k$ and $R_{w,g}'^k$ be the amount of spectrum allocated to AV k from $\beta_2\ R^{\max}$ and $\beta_w R^{\max}$, respectively, by Wi-Fi AP W_g under the coverage of eNB S_1 (i.e., $W_g \in \mathcal{A}_1$). Then the spectrum efficiencies at AV k from Wi-Fi AP W_g include the following two parts,

$$\begin{aligned} r_{2,g}'^k &= \log_2\Big(1 + \frac{P_g' G_g'^k}{\sum\limits_{W_i \in \mathcal{A}_1, i \neq g} P_i' G_i'^k + \sum\limits_{S_j \in \mathcal{B}_2} P_j G_j^k + \sigma^2}\Big) \\ r_{w,g}'^k &= \log_2\Big(1 + \frac{P_g' G_g'^k}{\sum\limits_{W_i \in \{\mathcal{A}_1 \cup \mathcal{A}_2\}, i \neq g} P_i' G_i'^k + \sigma^2}\Big). \end{aligned} \tag{3}$$

And the achievable transmission rate of a tagged AV k associated with Wi-Fi AP W_g, i.e., $k \in \cup_{W_g \in \mathcal{A}_1} \mathcal{N}_g$, can be expressed as

$$\gamma_g'^k = R_{2,g}'^k r_{2,g}'^k + R_{w,g}'^k r_{w,g}'^k. \tag{4}$$

Let $R_{1,h}'^k$ and $R_{w,h}'^k$ be the amount of spectrum allocated for AV k from $\beta_1\ R^{\max}$ and $\beta_w R^{\max}$, respectively, by Wi-Fi AP W_h under the coverage of eNB S_2 (i.e., $W_h \in \mathcal{A}_2$), and $r_{1,h}'^k$ and $r_{w,h}'^k$ be the spectrum efficiencies at AV k from Wi-Fi AP W_h. Similarly, the achievable transmission rate of a tagged AV k associated with Wi-Fi AP W_h, i.e., $k \in \cup_{W_h \in \mathcal{A}_2} \mathcal{N}_h$, can be given by

$$\gamma_h'^k = R_{1,h}'^k r_{1,h}'^k + R_{w,h}'^k r_{w,h}'^k. \tag{5}$$

III. Resource Management Scheme

We consider two kinds of traffic for each AV: delay-sensitive traffic and delay-tolerant traffic. Examples of AV's delay-sensitive traffic include rear-end collision avoidance

and platooning/convoying. The delay-tolerant traffic can be HD map information downloading and infotainment services. Denote p as the probability that an AV generates a delay-sensitive request. To accommodate the large amounts of data traffic generated by AVs while guaranteeing different QoS requirements for AV applications, designing efficient resource management schemes are very important.

For downlink transmission to accommodate AVs' delay-sensitive requests, the transmission delay from eNB S_j or Wi-Fi AP W_i should be guaranteed statically. Let L_s and λ_s be the size and the arrival rate of the delay-sensitive packet. From [30], the maximum delay requirement, $D_{\max}$, can be transformed to a lower bound of the required transmission rate to guarantee that the downlink transmission delay exceeding $D_{\max}$ at most with probability ϱ, which can be expressed as

$$\gamma_{\min} = -\frac{L_s \log\varrho}{D_{\max}\log(1-\log\varrho/(\lambda_s D_{\max}))}. \tag{6}$$

A. Spectrum Resource Allocation

To address complicated resource allocation, we will introduce a two-tier approach, including spectrum slicing among BSs and spectrum allocating among AVs, as following.

1) Spectrum Slicing Among BSs: Based on the dynamic spectrum management framework, the total available spectrum resources are sliced according to the ratio set $\{\beta_1, \beta_2, \beta_w\}$ for different BSs. The main concern for spectrum slicing is fairness among BSs. To this end, a logarithmic utility function, which is concave and with diminishing marginal utility [30], is considered to achieve a certain level of fairness among BSs.

For AV k within the coverages of Wi-Fi APs, binary variables x_j^k and $x_i'^k$ represent the BS-vehicle association patterns, where $x_j^k = 1$ (or $x_i'^k = 1$) means AV k is associated with eNB S_j (or Wi-Fi AP W_i), $x_j^k = 0$ (or $x_i'^k = 0$) otherwise. Denote $\overline{\mathcal{M}}_j/\overline{M}_j$ as the set/number of AVs within the coverage of eNB S_j while outside of Wi-Fi APs. Then, the utility for AV k associated to eNBs or Wi-Fi APs is

$$u_k = \begin{cases} u_1^k = \log(\gamma_1^k), & \text{if } k \in \overline{\mathcal{M}}_1 \cup \{k | x_1^k = 1\} \\ u_2^k = \log(\gamma_2^k), & \text{if } k \in \overline{\mathcal{M}}_2 \cup \{k | x_2^k = 1\} \\ u_g'^k = \log(\gamma_g'^k), & \text{if } k \in \mathcal{N}_g \cap \{k | x_g^k = 1\} \\ u_h'^k = \log(\gamma_h'^k), & \text{if } k \in \mathcal{N}_h \cap \{k | x_h^k = 1\}. \end{cases} \tag{7}$$

The aggregated network utility is defined as the summation of utility of each individual AV. Let $\mathbf{R} = \{R_1^k, R_2^k\}$ and $\mathbf{R}' = \{R_{2,g}'^k, R_{w,g}'^k, R_{1,h}'^k, R_{w,h}'^k\}$ be the matrices describing spectrum allocated to AVs by eNBs and by Wi-Fi APs, respectively. For given BS-vehicle association patterns with fixed transmit power of each Wi-Fi AP, the aggregated network-wide utility maximization problem can be given by

$$\mathbf{P1}: \max_{\substack{\beta_1,\beta_2,\beta_w \\ \mathbf{R},\mathbf{R}'}} \sum_{k\in\overline{\mathcal{M}}_1} u_1^k + \sum_{W_g}\sum_{k\in\mathcal{N}_g}(x_1^k u_1^k + x_g'^k u_g'^k) + \sum_{k\in\overline{\mathcal{M}}_2} u_2^k + \sum_{W_h}\sum_{k\in\mathcal{N}_h}(x_2^k u_2^k + x_h'^k u_h'^k) \tag{8}$$

$$\text{s.t.} \begin{cases} \beta_1, \beta_2, \beta_w \in [0,1] & \text{(8a)} \\ \beta_1 + \beta_2 + \beta_w = 1 & \text{(8b)} \\ \sum_{k\in\overline{\mathcal{M}}_1} R_1^k + \sum_{W_g}\sum_{k\in\mathcal{N}_g} x_1^k\ R_1^k = \beta_1\ R^{\max} & \text{(8c)} \\ \sum_{k\in\overline{\mathcal{M}}_2} R_2^k + \sum_{W_h}\sum_{k\in\mathcal{N}_h} x_2^k\ R_2^k = \beta_2\ R^{\max} & \text{(8d)} \\ \sum_{k\in\mathcal{N}_g} x_g'^k R_{l,g}'^k = \beta_l R^{\max}, \quad l \in \{2, w\} & \text{(8e)} \\ \sum_{k\in\mathcal{N}_h} x_h'^k R_{l,h}'^k = \beta_l R^{\max}, \quad l \in \{1, w\} & \text{(8f)} \\ R_1^k, R_2^k, R_{2,g}'^k, R_{w,g}'^k, R_{1,h}'^k, R_{w,h}'^k \geq 0. & \text{(8g)} \end{cases}$$

In problem (P1), the objective function is to maximize the aggregated network utility. Since β_1, β_2, and β_w are the only three slicing ratios, constraints (8a) and (8b) are considered in (P1). Constraints (8c)-(8g) indicate that spectrum resources allocated to AVs by a BS should be constrained by its available spectrum resources. According to problem (P1), each BS equally allocates the spectrum resources to AVs associated to it (will be discussed in detail in the next section). However, the downlink transmission rate required by an AV depends on its application request. For a BS with a fixed amount of available spectrum resources, equally allocating spectrum to AVs associated to it and simultaneously guaranteeing their heterogeneous QoS requirements will reduce the number of accommodated AVs. Thus, QoS constraints on $\mathbf{R}$ and $\mathbf{R}'$ are not considered in problem (P1) and the optimal $\{\beta_1^\star, \beta_2^\star, \beta_w^\star\}$ is regarded as the only output to slice the total spectrum resources among BSs.

2) Spectrum Allocating Among AVs: To accommodate situations with high density AVs, a linear network utility function is considered in allocating spectrum among AVs associated to the same BS. For given slicing ratios β_1, β_2, and β_w, and transmit power of each Wi-Fi AP, a network throughput maximization problem can be formulated as

$$\mathbf{P2}: \max_{\substack{\mathbf{X},\mathbf{X}' \\ \mathbf{R},\mathbf{R}'}} \sum_{k\in\overline{\mathcal{M}}_1} \gamma_1^k + \sum_{W_g\in\mathcal{A}_1}\sum_{k\in\mathcal{N}_g}(x_1^k\gamma_1^k + x_g'^k\gamma_g'^k) + \sum_{k\in\overline{\mathcal{M}}_2} \gamma_2^k + \sum_{W_h\in\mathcal{A}_2}\sum_{k\in\mathcal{N}_h}(x_2^k\gamma_2^k + x_h'^k\gamma_h'^k) \tag{9}$$

$$\text{s.t.} \begin{cases} \text{(8c)} - \text{(8g)} & \text{(9a)} \\ x_1^k, x_2^k, x_g'^k, x_h'^k \in \{0,1\}, & k \in \mathcal{N}_i \quad \text{(9b)} \\ x_1^k + x_g'^k = 1, & k \in \cup_{W_g}\mathcal{N}_g \quad \text{(9c)} \\ x_2^k + x_h'^k = 1, & k \in \cup_{W_h}\mathcal{N}_h \quad \text{(9d)} \\ \gamma_l^k \geq \gamma_{min}, \quad l \in \{1,2\}, k \in \{\overline{\mathcal{M}}_1^s \cup \overline{\mathcal{M}}_2^s\} & \text{(9e)} \\ x_1^k[\gamma_1^k - \gamma_{min}] \geq 0, & k \in \cup_{W_g}\mathcal{N}_g^s \quad \text{(9f)} \\ x_2^k[\gamma_2^k - \gamma_{min}] \geq 0, & k \in \cup_{W_h}\mathcal{N}_h^s \quad \text{(9g)} \\ x_i'^k[\gamma_i'^k - \gamma_{min}] \geq 0, & k \in \cup_{W_i\in\mathcal{A}_1\cup\mathcal{A}_2}\mathcal{N}_i^s \quad \text{(9h)} \\ \gamma_l^k \geq \lambda_n L_n, \quad l \in \{1,2\}, k \in \{\overline{\mathcal{M}}_1^t \cup \overline{\mathcal{M}}_2^t\} & \text{(9i)} \\ x_1^k[\gamma_1^k - \lambda_n L_n] \geq 0, & k \in \cup_{W_g}\mathcal{N}_g^t \quad \text{(9j)} \\ x_2^k[\gamma_2^k - \lambda_n L_n] \geq 0, & k \in \cup_{W_h}\mathcal{N}_g^t \quad \text{(9k)} \\ x_i'^k[\gamma_i'^k - \lambda_n L_n] \geq 0, & k \in \cup_{W_i\in\mathcal{A}_1\cup\mathcal{A}_2}\mathcal{N}_i^t \quad \text{(9l)} \end{cases}$$

where $\mathbf{X} = \{x_1^k, x_2^k\}$ and $\mathbf{X}' = \{x_g'^k, x_h'^k\}$ are the association pattern matrices between eNBs and AVs, and between Wi-Fi APs and AVs, respectively; L_n and λ_n are the corresponding packet size and the arrival rate for delay-tolerant service requests; $\overline{\mathcal{M}}_j^s/\overline{M}_j^s$ (or $\overline{\mathcal{M}}_j^t/\overline{M}_j^t$) are the set/number of AVs only within the coverage of eNB S_j and requesting for delay-sensitive (or delay-tolerant) services; $\mathcal{N}_i^s/N_i^s$ (or $\mathcal{N}_i^t/N_i^t$) are the set/number of AVs within the coverage of Wi-Fi AP W_i and requesting for delay-sensitive (or delay-tolerant) services.

In problem (P2), the first five constraints are same with problem (P1) and used to demonstrate the required spectrum for each AV allocated by its associated BS. Constraints (9b)-(9d) indicate that each AV is associated with either the eNB or the Wi-Fi AP closed to it. Constraints (9e)-(9h) ensure the service rates from eNBs and Wi-Fi APs to guarantee the delay requirements of delay-sensitive services. For AVs with delay-tolerant requests, constraints (9i)-(9l) indicate that the service rate from an eNB or a Wi-Fi AP should be not less than the periodic data traffic arrival rate at that eNB or Wi-Fi AP. Via solving problem (P2), the optimal association pattern matrices $\mathbf{X}^*$ and $\mathbf{X}^{*\prime}$, and local spectrum allocation matrices $\mathbf{R}^*$ and $\mathbf{R}^{*\prime}$ can be obtained, which maximize the network throughput with guaranteed QoS for different AV applications.

B. Transmit Power Control

In addition to spectrum slicing and allocating among BSs and among AVs, controlling the transmit power of Wi-Fi APs to adjust the inter-cell interference would further improve the spectrum utilization. Denote $\mathbf{P}' = \{P_i' | W_i \in \mathcal{A}_1 \cup \mathcal{A}_2\}$ as the transmit power matrix of Wi-Fi APs. Equations (1) and (3) indicate that the received signal-to-interference-plus-noise (SINR) [31] by AVs from either an eNB or a Wi-Fi AP change with Wi-Fi APs' transmit powers, and therefore, impacting the achievable transmission rates of the corresponding downlink. To obtain optimal transmit powers of Wi-Fi APs, the linear utility function is considered in this part similar to problem (P2). For a given slicing ratio set $\{\beta_1, \beta_2, \beta_w\}$, BS-vehicle association pattern matrices $\mathbf{X}$ and $\mathbf{X}'$, and local spectrum allocation matrices $\mathbf{R}$ and $\mathbf{R}'$, the network throughput maximization problem focusing on transmit power controlling can be formulated as

$$\mathbf{P3}: \max_{\mathbf{P}'} \sum_{k\in\overline{\mathcal{M}}_1} \gamma_1^k + \sum_{W_g\in\mathcal{A}_1}\sum_{k\in\mathcal{N}_g}(x_1^k\gamma_1^k + x_g'^k\gamma_g'^k) + \sum_{k\in\overline{\mathcal{M}}_2}\gamma_2^k + \sum_{W_h\in\mathcal{A}_2}\sum_{k\in\mathcal{N}_h}(x_2^k\gamma_2^k + x_h'^k\gamma_h'^k) \quad (10)$$

$$\text{s.t.} \begin{cases} (9e)-(9l), & (10a) \\ P_i' \in [0, P^{\max}], \quad W_i \in \{\mathcal{A}_1 \cup \mathcal{A}_2\} & (10b) \end{cases}$$

where $P^{\max}$ is the maximum transmit power allowed by each Wi-Fi AP. In problem (P3), the first eight constraints in (10a) are same with problem (P2) and used to ensure the QoS requirements for delay-sensitive and delay-tolerant services. Constraint (10b) indicates that transmit power of each Wi-Fi AP is less than $P^{\max}$. Then the optimal transmit power for each Wi-Fi AP can be determined by solving problem (P3). From the above discussion, variables considered in problems (P1), (P2), and (P3) are coupled, thus the three problems should be solved jointly.

IV. Problem Analysis and Suboptimal Solution

In this section, we first analyze each problem and then transform (P2) and (P3) to tractable forms before we jointly solving these three problems for the final optimal solutions.

A. Problem Analysis

Let $\mathcal{N}_i'$ be the set of AVs within and associated with Wi-Fi AP W_i, i.e., $\mathcal{N}_i' = \{k \in \mathcal{N}_i | x_i'^k = 1\}$ for $W_i \in \{\mathcal{A}_1 \cup \mathcal{A}_2\}$, and $|\mathcal{N}_i'| = N_i'$. Then, the objective function of (P1) can be transformed into,

$$\sum_{k\in\{\mathcal{M}_1\setminus(\cup_{W_g}\mathcal{N}_g')\}} \log(R_1^k\ r_1^k) + \sum_{W_g}\sum_{k\in\mathcal{N}_g'}\log(\gamma_g'^k) + \sum_{k\in\{\mathcal{M}_2\setminus(\cup_{W_h}\mathcal{N}_h')\}} \log(R_2^k\ r_2^k) + \sum_{W_h}\sum_{k\in\mathcal{N}_h'}\log(\gamma_h'^k) \quad (11)$$

where mathematical symbol, \, describes the relative complement of one set with respect to another set. According to the constraints of (P1), the sets of spectrum allocation variables, $\{R_1^k\}$, $\{R_2^k\}$, $\{R_{2,g}'^k\}$, $\{R_{w,g}'^k\}$, $\{R_{1,h}'^k\}$, and $\{R_{w,h}'^k\}$, are independent with uncoupled constrains. Thus, similar to proposition 1 in [30], we can decompose problem (P1) into six subproblems and obtain the optimal fractions of spectrum allocated to AVs from the associated BSs as follows,

$$\begin{aligned} R_1^* &= R_1^{*k} = \frac{\beta_1 R^{\max}}{M_1 - \sum_{W_g} N_g'} \\ R_2^* &= R_2^{*k} = \frac{\beta_2 R^{\max}}{M_2 - \sum_{W_h} N_h'} \\ R_{2,g}^{*\prime} &= R_{2,g}^{*\prime k} = \frac{\beta_2 R^{\max}}{N_g'} \\ R_{w,g}^{*\prime} &= R_{w,g}^{*\prime k} = \frac{\beta_w R^{\max}}{N_g'} \\ R_{1,h}^{*\prime} &= R_{1,h}^{*\prime k} = \frac{\beta_1 R^{\max}}{N_h'} \\ R_{w,h}^{*\prime} &= R_{w,h}^{*\prime k} = \frac{\beta_w R^{\max}}{N_h'}. \end{aligned} \quad (12)$$

Equation (12) indicates that each BS equally allocates spectrum to AVs associated to it. By replacing the spectrum allocation variables with Equation (12), problem (P1) can be transformed into

$$\begin{aligned} \mathbf{P1}': \max_{\beta_1,\beta_2,\beta_w} & \sum_{k\in\{\mathcal{M}_1\setminus(\cup_{W_g}\mathcal{N}_g')\}} \log\left(\frac{\beta_1\ R^{\max} r_1^k}{M_1 - \sum_{W_g} N_g'}\right) \\ & + \sum_{W_g}\sum_{k\in\mathcal{N}_g'} \log\left(\frac{\beta_2\ R^{\max} r_{2,g}'^k + \beta_w R^{\max} r_{w,g}'^k}{N_g'}\right) \\ & + \sum_{k\in\{\mathcal{M}_2\setminus(\cup_{W_h}\mathcal{N}_h')\}} \log\left(\frac{\beta_2\ R^{\max} r_2^k}{M_2 - \sum_{W_h} N_h'}\right) \\ & + \sum_{W_h}\sum_{k\in\mathcal{N}_h'} \log\left(\frac{\beta_1 R^{\max} r_{1,h}'^k + \beta_w R^{\max} r_{w,h}'^k}{N_h'}\right) \end{aligned} \quad (13)$$

$$\text{s.t.}\{\ (8a)-(8b). \quad (13a)$$

Due to the binary variable matrices $\mathbf{X}$ and $\mathbf{X}'$, using the brute force algorithm to solve problems (P2) and (P3) is with high complexity. To address this issue, we allow AVs within the overlapping area of a Wi-Fi AP and an eNB to associate to one or both of the Wi-Fi AP and the eNB [32]. Thus, binary matrices $\mathbf{X}$ and $\mathbf{X}'$ are relaxed into real-valued matrices $\widetilde{\mathbf{X}}$ and $\widetilde{\mathbf{X}}'$ with elements $\widetilde{x}_j^k \in [0,1]$ and $\widetilde{x}_i'^k \in [0,1]$, respectively. And then, we can transform problem (P2) into

$$\mathbf{P2}': \max_{\substack{\widetilde{\mathbf{X}},\widetilde{\mathbf{X}}'\\ \mathbf{R},\mathbf{R}'}} \sum_{k\in\overline{\mathcal{M}}_1} \gamma_1^k + \sum_{W_g\in\mathcal{A}_1}\sum_{k\in\mathcal{N}_g}(\widetilde{x}_1^k\gamma_1^k + \widetilde{x}_g'^k\gamma_g'^k) + \sum_{k\in\overline{\mathcal{M}}_2}\gamma_2^k + \sum_{W_h\in\mathcal{A}_2}\sum_{k\in\mathcal{N}_h}(\widetilde{x}_2^k\gamma_2^k + \widetilde{x}_h'^k\gamma_h'^k) \quad (14)$$

$$\text{s.t.}\begin{cases} \sum_{k\in\overline{\mathcal{M}}_1} R_1^k + \sum_{W_g}\sum_{k\in\mathcal{N}_g}\widetilde{x}_1^k\ R_1^k = \beta_1\ R^{\max} & (14a)\\ \sum_{k\in\overline{\mathcal{M}}_2} R_2^k + \sum_{W_h}\sum_{k\in\mathcal{N}_h}\widetilde{x}_2^k\ R_2^k = \beta_2\ R^{\max} & (14b)\\ \sum_{k\in\mathcal{N}_g}\widetilde{x}_g'^k R_{l,g}'^k = \beta_l R^{\max}, \quad l\in\{2,w\} & (14c)\\ \sum_{k\in\mathcal{N}_h}\widetilde{x}_h'^k R_{l,h}'^k = \beta_l R^{\max}, \quad l\in\{1,w\} & (14d)\\ R_1^k, R_2^k, R_{2,g}'^k, R_{w,g}'^k, R_{1,h}'^k, R_{w,h}'^k \geq 0 & (14e)\\ \widetilde{x}_1^k, \widetilde{x}_2^k, \widetilde{x}_g'^k, \widetilde{x}_h'^k \in [0,1], \quad k\in\mathcal{N}_i & (14f)\\ \widetilde{x}_1^k + \widetilde{x}_g'^k = 1, \quad k\in\cup_{W_g}\mathcal{N}_g & (14g)\\ \widetilde{x}_2^k + \widetilde{x}_h'^k = 1, \quad k\in\cup_{W_h}\mathcal{N}_h & (14h)\\ \gamma_l^k \geq \gamma_{min}, \quad l\in\{1,2\}, k\in\{\overline{\mathcal{M}}_1^s\cup\overline{\mathcal{M}}_2^s\} & (14i)\\ \widetilde{x}_1^k[\gamma_1^k - \gamma_{min}]\geq 0, \quad k\in\cup_{W_g}\mathcal{N}_g^s & (14j)\\ \widetilde{x}_2^k[\gamma_2^k - \gamma_{min}]\geq 0, \quad k\in\cup_{W_h}\mathcal{N}_h^s & (14k)\\ \widetilde{x}_i'^k[\gamma_i'^k - \gamma_{min}]\geq 0, \quad k\in\cup_{W_i\in\mathcal{A}_1\cup\mathcal{A}_2}\mathcal{N}_i^s & (14l)\\ \gamma_l^k \geq \lambda_n L_n, \quad l\in\{1,2\}, k\in\{\overline{\mathcal{M}}_1^t\cup\overline{\mathcal{M}}_2^t\} & (14m)\\ \widetilde{x}_1^k[\gamma_1^k - \lambda_n L_n]\geq 0, \quad k\in\cup_{W_g}\mathcal{N}_g^t & (14n)\\ \widetilde{x}_2^k[\gamma_2^k - \lambda_n L_n]\geq 0, \quad k\in\cup_{W_h}\mathcal{N}_g^t & (14o)\\ \widetilde{x}_i'^k[\gamma_i'^k - \lambda_n L_n]\geq 0, \quad k\in\cup_{W_i\in\mathcal{A}_1\cup\mathcal{A}_2}\mathcal{N}_i^t. & (14p)\end{cases}$$

To analyze the concavity property of problems (P1′) and (P2′), three definitions about concave functions [33], [34] and two concavity-preserving operations [33] are introduced in Appendix A. The following propositions, proved in Appendix B and Appendix C, summarize the concavity property of problems (P1′) and (P2′), respectively,

Proposition 1: The objective function of problem (P1′) is a concave function on the three optimal variables β_1, β_2, and β_w, and problem (P1′) is a concave optimization problem.

Proposition 2: The objective function of problem (P2′) is a biconcave function on variable set $\{\widetilde{\boldsymbol{X}},\widetilde{\boldsymbol{X}}'\}\times\{\boldsymbol{R},\boldsymbol{R}'\}$, and problem (P2′) is a biconcave optimization problem.

Even though the integer-value variables in problem (P3) can be relaxed to real-value ones by replacing constraint (10a) by (14i)-(14p), the non-concave or non-biconcave relations between the objective function and decision variable of problem (P3) makes it difficult to solve directly. Thus, we use the first-order Taylor series approximation, and introduce two new variable matrices, $\mathbf{C} = \{C_1^k, C_2^k\}$ and $\mathbf{C}' = \{C_{2,g}'^k, C_{w,g}'^k, C_{1,h}'^k, C_{w,h}'^k\}$ with elements that are linear-fractional function of P_i', to replace the received SINR on AVs within each BS's coverage. Then, the downlink spectrum efficiency on an AV associated to a BS can be re-expressed as a concave function of C. For example, using C_1^k to replace the SINR received on AV k associated to eNB S_1, we can rewritten equation (1) as

$$r_1^k = \log_2(1 + C_1^k). \quad (15)$$

Therefore, problem (P3) can be transformed into

$$\mathbf{P3}': \max_{\mathbf{P}',\mathbf{C},\mathbf{C}'} \sum_{k\in\overline{\mathcal{M}}_1} R_1^k\log_2(1+C_1^k) + \sum_{k\in\overline{\mathcal{M}}_2} R_2^k\log_2(1+C_2^k) + \sum_{W_g\in\mathcal{A}_1}\sum_{k\in\mathcal{N}_g}(x_1^k R_1^k\log_2(1+C_1^k) + x_g'^k(R_{2,g}'^k\log_2(1+C_{2,g}'^k) + R_{w,g}'^k\log_2(1+C_{w,g}'^k))) + \sum_{W_h\in\mathcal{A}_2}\sum_{k\in\mathcal{N}_h}(x_2^k R_2^k\log_2(1+C_2^k) + x_h'^k(R_{1,h}'^k \log_2(1+C_{1,h}'^k) + R_{w,h}'^k\log_2(1+C_{w,h}'^k))) \quad (16)$$

$$\text{s.t.}\begin{cases} (14\text{i}) - (14\text{p}) & (16a)\\ P_i' \in [0, P^{\max}], \quad W_i\in\{\mathcal{A}_1\cup\mathcal{A}_2\} & (16b)\\ C_1^k \leq \xi_1^k & (16c)\\ C_2^k \leq \xi_2^k & (16d)\\ C_{2,g}'^k \leq \xi_{2,g}'^k & (16e)\\ C_{w,g}'^k \leq \xi_{w,g}'^k & (16f)\\ C_{1,h}'^k \leq \xi_{1,h}'^k & (16g)\\ C_{w,h}'^k \leq \xi_{w,h}'^k & (16h)\end{cases}$$

where ξ^k (or ξ'^k) are the received SINRs on AV k from its associated eNB (or Wi-Fi AP). The six additional constraints (16c)-(16h) are biaffine on $\{\mathbf{P}'\}\times\{\mathbf{C},\mathbf{C}'\}$ and are considered in problem (P3′) to ensure the equivalent with problems (P3).

B. Algorithms Design

To jointly solve the three problems (P1′), (P2′), and (P3′), we first design an alternate algorithm for (P3′) and then an *alternate concave search* (ACS) algorithm is applied to jointly solve these three problems. For simplicity, the objective functions for the three problems are denoted by $\mathcal{U}_{(P1')}$, $\mathcal{U}_{(P2')}$, and $\mathcal{U}_{(P3')}$, respectively.

The objective function of problem (P3′), $\mathcal{U}_{(P3')}$, is concave on $\{\mathbf{C},\mathbf{C}'\}$, while constraints (16c)-(16h) are biaffine on $\{\mathbf{P}'\}\times\{\mathbf{C},\mathbf{C}'\}$. Through maximizing $\mathcal{U}_{(P3')}$, optimal $\{\mathbf{C},\mathbf{C}'\}$ can be obtained for given $\mathbf{P}'$ with constraints (16c)-(16h). Moreover, through maximizing 0 with constraints (16a)-(16h), the feasible set of $\mathbf{P}'$ can be obtained. Thus, we first separate problem (P3′) into two subproblems as follows

$$\mathbf{P3}'.\mathbf{SP1}: \max_{\mathbf{C},\mathbf{C}'}\ \mathcal{U}_{(P3')} \quad \text{s.t. } (16c) - (16h)$$

and

$$\mathbf{P3'.SP2}: \max_{\mathbf{P'}} \ 0 \quad \text{s.t. } (16a)-(16h).$$

It is obvious that there must be a solution to subproblem (P3′.SP1). Moreover, since subproblem (P3′.SP2) is a feasibility problem and the initial value of $\mathbf{P}'$ is always the solution for (P3′.SP2). Thus, problem (P3′) converges and can be solved by iteratively solving subproblems (P3′.SP1) and (P3′.SP2).

To jointly solve (P1′), (P2′), and (P3′) and obtain the final optimal decision variables, the ACS algorithm is summarized in Algorithm 1. $\{\widetilde{\mathbf{X}}^{(t)}, \widetilde{\mathbf{X}}^{(t)\prime}\}$ and $\mathbf{P}^{(t)\prime}$ are the values of $\{\widetilde{\mathbf{X}}, \widetilde{\mathbf{X}}'\}$ and $\mathbf{P}'$ at the beginning of the tth iteration, and $\mathcal{U}^{(t)}_{(P2')}$ is the maximum objective function value of problem (P2′) with optimal decision variables $\{\beta_1^{(t)}, \beta_2^{(t)}, \beta_w^{(t)}\}$, $\{\widetilde{\mathbf{R}}^{(t)}, \widetilde{\mathbf{R}}^{(t)\prime}\}$, $\{\widetilde{\mathbf{X}}^{(t)}, \widetilde{\mathbf{X}}^{(t)\prime}\}$, and $\mathbf{P}^{(t)\prime}$. To enhance the convergence speed of Algorithm 1, the output at the $(t-1)$th iteration is regarded as a feedback to the input at the tth iteration [35], such as, the tth input $\mathbf{P}^{(t)\prime}$ is defined as

$$\mathbf{P}^{(t)\prime} = \mathbf{P}^{(t-1)\prime} + \theta(\mathbf{P}^{\dagger\prime} - \mathbf{P}^{(t-1)\prime}) \tag{17}$$

where, θ is the feedback coefficient. Moreover, considering that a lager θ may result in missing optimal output at each iteration while a small θ reduces the convergence speed, two coefficients θ_1 and θ_2 are considered in Algorithm 1.

According to the analysis of each problem in subsection IV-A, Algorithm 1 converges since:

(i) The output of problems (P1′) and (P2′), $\{\beta_1, \beta_2, \beta_w\}$, $\{\widetilde{\mathbf{X}}, \widetilde{\mathbf{X}}'\}$, and $\{\widetilde{\mathbf{R}}, \widetilde{\mathbf{R}}'\}$, are closed sets;
(ii) Both (P1′) and (P2′) are concave/biconcave optimization problems such that the optimal solution for each problem at the end of the kth iteration is unique when the input of the algorithm is the optimal results obtained from the $(k-1)$th iteration;
(iii) Problem (P3′) is always solvable.

V. Simulation Results

To show the effectiveness of our proposed spectrum resource management framework, extensive simulation is carried out. We compare the proposed spectrum resource management scheme with two existing resource slicing schemes, i.e., the maximization-utility (max-utility) based resource slicing scheme proposed in [30], and the maximization-SINR (max-SINR) based resource slicing scheme proposed in [32]. The BS-vehicle association patterns and spectrum slicing ratios are optimized with objective of maximizing the aggregated network utility in max-utility scheme while AVs choose to associate with the BS providing higher SINR and only spectrum slicing ratios are optimized in max-SINR scheme.

We consider two eNBs (eNB $S_1 \in \mathcal{B}_1$ and eNB $S_2 \in \mathcal{B}_2$) and four Wi-Fi APs (AP 1 and AP 2 in $\mathcal{A}_1$, and AP 3 and AP 4 in $\mathcal{A}_2$) are utilized for AV applications. Transmit power is fixed at 10 watts (i.e., 40 dBm) for each eNB with a maximum communication range of 600 m. Since no transmit power control for both of max-utility and max-SINR schemes, transmit powers of APs are set as 1 watt with communication range of 200 m, the same as in [30]. In our simulation, the minimum inter-vehicle distance is 5 m, and the AV density over one lane, i.e., the number of AVs on one lane per meter,

Algorithm 1 The ACS Algorithm for Jointly Solving (P1′), (P2′), and (P3′)

Input: Input parameters for (P1′), (P2′), and (P3′); initial values for $\{\widetilde{\mathbf{X}}, \widetilde{\mathbf{X}}'\}$ and $\mathbf{P}'$; terminating criterion κ_1; feedback coefficient updating criterion κ_2 ($\kappa_2 > \kappa_1$); feedback coefficients θ_1 and θ_2; maximum iterations $\widehat{N}$.
Output: Optimal spectrum slicing ratios, $\{\beta_1^*, \beta_2^*, \beta_w^*\}$; Optimal local spectrum allocation matrix, $\{\mathbf{R}^*, \mathbf{R}^{*\prime}\}$; Optimal BS-vehicle association patterns, $\{\widetilde{\mathbf{X}}^*, \widetilde{\mathbf{X}}^{*\prime}\}$; Optimal transmit powers for APs, $\mathbf{P}^{*\prime}$; Optimal SINR matrices $\{\mathbf{C}^*, \mathbf{C}^{*\prime}\}$.

/* Initialization phase */
for *the first iteration,* $k = 0$ **do**
  set initial values for $\{\widetilde{\mathbf{X}}, \widetilde{\mathbf{X}}'\}$ and $\mathbf{P}'$, denoted by $\{\widetilde{\mathbf{X}}^{(0)}, \widetilde{\mathbf{X}}^{(0)\prime}\}$ and $\mathbf{P}^{(0)\prime}$, respectively; set $\mathcal{U}^{(0)}_{(P2')}$ to 0.
/* Solving iteratively phase */
repeat
  foreach $k \le \widehat{N}$ **do**
    Step1: $\{\beta_1^\dagger, \beta_2^\dagger, \beta_w^\dagger\} \leftarrow$ solving (P1′) given $\{\widetilde{\mathbf{X}}^{(t)}, \widetilde{\mathbf{X}}^{(t)\prime}\}$ and $\mathbf{P}^{(t)\prime}$;
    Step2: $\{\mathbf{R}^\dagger, \mathbf{R}^{\dagger\prime}\} \leftarrow$ solving (P2′) given $\{\beta_1^\dagger, \beta_2^\dagger, \beta_w^\dagger\}$, $\{\widetilde{\mathbf{X}}^{(t)}, \widetilde{\mathbf{X}}^{(t)\prime}\}$, and $\mathbf{P}^{(t)\prime}$;
    Step3: $\{\widetilde{\mathbf{X}}^\dagger, \widetilde{\mathbf{X}}^{\dagger\prime}\} \leftarrow$ solving (P2′) given $\{\beta_1^\dagger, \beta_2^\dagger, \beta_w^\dagger\}$, $\{\mathbf{R}^\dagger, \mathbf{R}^{\dagger\prime}\}$, and $\mathbf{P}^{(t)\prime}$;
    Step4: $\{\mathbf{C}^{(t+1)}, \mathbf{C}^{(t+1)\prime}\}$, $\mathbf{P}^{(t+1)\prime} \leftarrow$ solving (P3′) by iteratively solving (P3′.SP1) and (P3′.SP2) given $\{\beta_1^\dagger, \beta_2^\dagger, \beta_w^\dagger\}$, $\{\mathbf{R}^\dagger, \mathbf{R}^{\dagger\prime}\}$, and $\{\widetilde{\mathbf{X}}^\dagger, \widetilde{\mathbf{X}}^{\dagger\prime}\}$;
    if *No feasible solutions for (P1′), (P2′), or (P3′)* **then**
      Go to initialization phase and reset the initial values for related parameters until no feasible solutions found; Stop and no optimal solutions under current network setting;
    else if $\| \mathcal{U}^{(t)}_{(P2')} - \mathcal{U}^{(t-1)}_{(P2')} \| \le \kappa_2$ **then**
      $\{\beta_1^{(t+1)}, \beta_2^{(t+1)}, \beta_w^{(t+1)}\} \leftarrow \{\beta_1^{(t)}, \beta_2^{(t)}, \beta_w^{(t)}\} + \theta_2 * (\{\beta_1^\dagger, \beta_2^\dagger, \beta_w^\dagger\} - \{\beta_1^{(t)}, \beta_2^{(t)}, \beta_w^{(t)}\})$;
      $\{\mathbf{R}^{(t+1)}, \mathbf{R}^{(t+1)\prime}\} \leftarrow \{\mathbf{R}^{(t)}, \mathbf{R}^{(t)\prime}\} + \theta_2 * (\{\mathbf{R}^\dagger, \mathbf{R}^{\dagger\prime}\} - \{\mathbf{R}^{(t)}, \mathbf{R}^{(t)\prime}\})$;
      $\{\mathbf{X}^{(t+1)}, \mathbf{X}^{(t+1)\prime}\} \leftarrow \{\mathbf{X}^{(t)}, \mathbf{X}^{(t)\prime}\} + \theta_2 * (\{\mathbf{X}^\dagger, \mathbf{X}^{\dagger\prime}\} - \{\mathbf{X}^{(t)}, \mathbf{X}^{(t)\prime}\})$.
    else
      $\{\beta_1^{(t+1)}, \beta_2^{(t+1)}, \beta_w^{(t+1)}\} \leftarrow \{\beta_1^{(t)}, \beta_2^{(t)}, \beta_w^{(t)}\} + \theta_1 * (\{\beta_1^\dagger, \beta_2^\dagger, \beta_w^\dagger\} - \{\beta_1^{(t)}, \beta_2^{(t)}, \beta_w^{(t)}\})$;
      $\{\mathbf{R}^{(t+1)}, \mathbf{R}^{(t+1)\prime}\} \leftarrow \{\mathbf{R}^{(t)}, \mathbf{R}^{(t)\prime}\} + \theta_1 * (\{\mathbf{R}^\dagger, \mathbf{R}^{\dagger\prime}\} - \{\mathbf{R}^{(t)}, \mathbf{R}^{(t)\prime}\})$;
      $\{\mathbf{X}^{(t+1)}, \mathbf{X}^{(t+1)\prime}\} \leftarrow \{\mathbf{X}^{(t)}, \mathbf{X}^{(t)\prime}\} + \theta_1 * (\{\mathbf{X}^\dagger, \mathbf{X}^{\dagger\prime}\} - \{\mathbf{X}^{(t)}, \mathbf{X}^{(t)\prime}\})$.
    Obtain $\mathcal{U}^{(t+1)}_{(P2')}$ at the end of kth iteration with $\{\beta_1^{(t+1)}, \beta_2^{(t+1)}, \beta_w^{(t+1)}\}$, $\{\widetilde{\mathbf{R}}^{(t+1)}, \widetilde{\mathbf{R}}^{(t+1)\prime}\}$, $\{\widetilde{\mathbf{X}}^{(t+1)}, \widetilde{\mathbf{X}}^{(t+1)\prime}\}$, and $\mathbf{P}^{(t+1)\prime}$;
  $k \leftarrow k+1$;
until $\| \mathcal{U}^{(t)}_{(P2')} - \mathcal{U}^{(t-1)}_{(P2')} \| \le \kappa_1$ *or* $k \ge \widehat{N}$;

TABLE I
PARAMETERS VALUES

Parameter	Value
Maximum transmit power allowed by APs	2.5 watts
Background noise power	-104 dBm
HD map packet arrival rate	20 packet/s
HD map packet size	9000 bits
Safety-sensitive packet arrival rate	4 packet/s
Safety-sensitive packet size	1048 bits
Safety-sensitive packet delay bound	10 ms
Safety-sensitive request generating probability	$0.1 - 0.9$
Delay bound violation probability	10^{-3}
θ_1/θ_2	0.001/0.1
κ_1/κ_2	0.01/20

varies within range of [0.04, 0.20] AV/m. The downlink channel gains for eNBs and Wi-Fi APs are described as $L_e(d) = -30 - 35\log_{10}(d)$ and $L_w(d) = -40 - 35\log_{10}(d)$ [30], respectively, where d is the distance between an AV and a BS. We take platooning/convoying as an example to set the delay bound for delay-sensitive applications, i.e., 10 ms [8], [36], and downloading HD map is considered as an example for delay-tolerant applications [14]. Other important parameters in our simulation are listed in Table I.

We use network throughput that is, the summation of achievable transmission rate by each individual AV from BSs, to measure performances of different spectrum resource management schemes. Considering the scarcity of spectrum resources, the different AV applications, and the high network dynamic, we evaluate the performance of the proposed scheme and compare with the max-utility and the max-SINR schemes under different amounts of aggregate spectrum resource (W_v), probabilities of generating a delay-sensitive request by AVs (p), and AV densities in Fig. 3 to Fig. 5.

Fig. 3 demonstrates the network throughputs achieved by the three schemes with respect to different amounts of aggregate spectrum resources, W_v, where AV density is 0.05 AV/m and $p = 0.2$ and 0.8, respectively. With the increasing of W_v, transmission rate for each AV is increased due to the increasing of the amount of allocated spectrum resources. From Fig. 3, the minimum requirement for spectrum resources by the proposed scheme to support the downlink transmissions is 3 MHz while at least 9 MHz and 12 MHz spectrum are required by the max-utility scheme and the max-SINR scheme, respectively. Moreover, under different W_v, the network throughput achieved by the proposed scheme is on average over 70% and over 50% higher than that of the max-utility scheme for $p = 0.2$ and 0.8, respectively, and over 45% higher on average than that of the max-SINR scheme for $p = 0.2$. From Fig. 3(a), with the increase of W_v, network throughput achieved by the proposed scheme increases more rapidly than the max-utility scheme.

Network throughputs of the three schemes under different p are evaluated in Fig. 4. The effect of p on network throughput is mainly caused by the difference between the QoS requirements for delay-sensitive and delay-tolerant applications. According to Equation (6) and the parameter setting in Table I, the transmission rate required by a delay-tolerant request is 180.00 kbits/s, which is higher than that

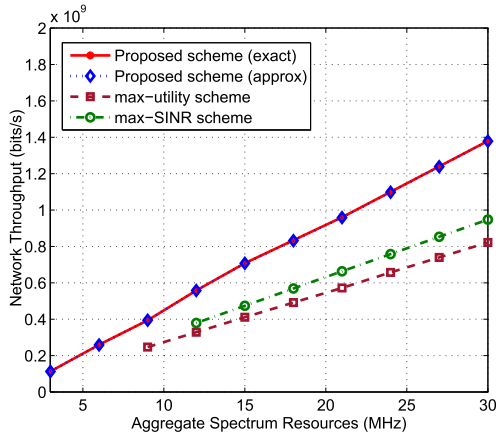

(a)

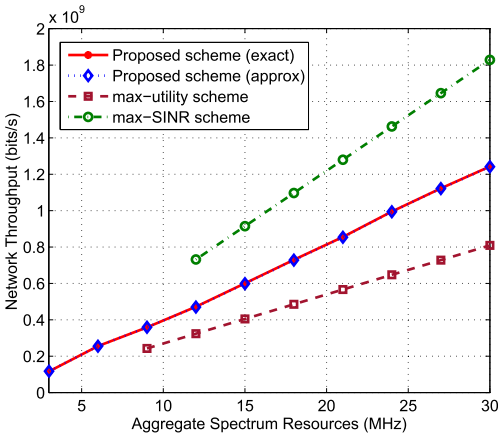

(b)

Fig. 3. Comparison of network throughput vs. aggregate spectrum resources under the same AV distribution with AV density 0.05AV/m. (a) $p = 0.2$. (b) $p = 0.8$.

for a delay-sensitive request, 140.37 kbits/s. A large p indicates a low total transmission rate required by all AVs to satisfy their applications' QoS requirements, therefore more remaining spectrum resources can be allocated to AVs with higher received SINRs in the proposed scheme. Thus, under the scenarios with the same AV density, 0.05 AV/m, network throughputs of the three schemes increase with p. For the max-SINR scheme, AVs associate the BS providing higher SINR and each BS equally allocates its available spectrum resources to AVs. To guarantee the QoS requirements for AVs, the amount of spectrum resource allocated to AVs from the same BS fluctuates with the distribution of BS-vehicle SINR and p, resulting in drastic impacts on the achieved network throughput. Moreover, from Fig. 4, the proposed scheme outperforms the max-SINR scheme when p is small and can achieve higher network throughput than the max-utility scheme for the scenario with different p.

Fig. 5 shows the network throughputs of the three schemes under different AV densities with $p = 0.2$ and 0.8, respectively, and 20 MHz aggregate spectrum resources. From the figure, the proposed scheme is more robust to AV density changing than the other two. For both the max-SINR and the max-utility schemes, only scenarios with small AV densities

TABLE II
OPTIMAL TRANSMIT POWERS AND NUMBER OF ITERATIONS FOR THE THREE SCHEMES ($p = 0.8$)

AV Density (AV/m)	Optimal Transmit Powers P′(watts)				Number of Iterations		
	P_1'	P_2'	P_3'	P_4'	Proposed Scheme	max-utility Scheme	max-SINR Scheme
0.05	2.500	2.4054	2.4144	2.500	12	7	N/A
0.10	2.500	2.3840	2.3748	2.500	23	N/A	N/A
0.15	2.500	2.3761	2.3731	2.500	34	N/A	N/A
0.20	2.500	2.3699	2.3699	2.500	51	N/A	N/A

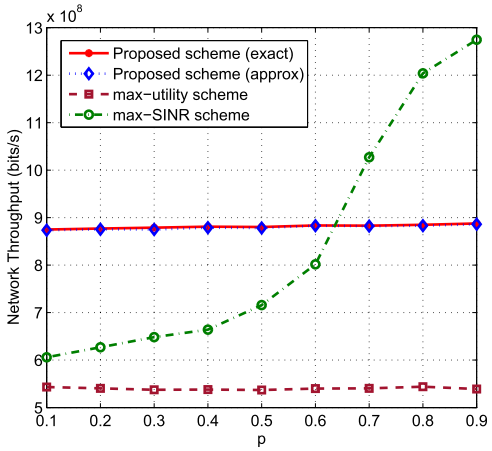

Fig. 4. Average network throughput vs. p (AV density is 0.05AV/m).

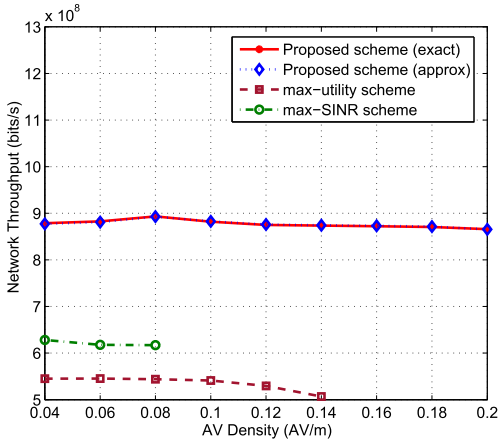

(a)

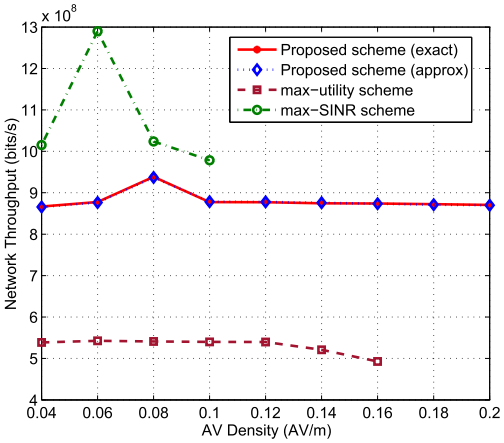

(b)

Fig. 5. Average network throughput vs. AV density. (a) $p = 0.2$. (b) $p = 0.8$.

can be accommodated due to equal spectrum allocation among AVs and unbalance between the downlink data traffic and the available aggregate spectrum resources. Furthermore, the proposed scheme has over 50% increase in the achieved network throughput than the max-utility scheme with $p = 0.2$ and 0.8 and has over 40% increase than the max-SINR scheme when $p = 0.2$.

Fig. 5 also indicates the effect of AV density on the achieved network throughputs by the three schemes. In general, the network throughputs achieved by the three schemes overall decrease with AV density. To increase the network throughput, the proposed scheme and the max-SINR scheme prefer to slicing high spectrum ratio to the BSs providing higher SINRs to its associated AVs once enough spectrum is allocated to each AV to guarantee the QoS requirements for their applications. When the AV density is relatively lower (e.g., 0.04 AV/m), 20 MHz spectrum resource is more than enough to satisfy each request's QoS requirement and the average probability for AVs with high SINR increases with the AV density, therefore resulting in increasing network throughput. However, the amount of spectrum resources needed to satisfy AV application's QoS requirements increases with the AV density for the three schemes, thus less spectrum resources can be used for increasing network throughput, resulting in decreasing in network throughput.

Fig. 3 to Fig. 5 show that the proposed scheme outperforms the two comparisons in terms of network throughput. In addition to replacing the equality allocation with on-demand spectrum allocation among AVs, the performance improving is also due to the transmit power controlling in the proposed scheme. Taking scenarios with four different AV densities, i.e., 0.05 AV/m, 0.10 AV/m, 0.15 AV/m, and 0.20 AV/m, as examples, the optimal transmit powers obtained by the proposed scheme are shown in Table II. To avoid the impact of the initial APs' transmit powers on the network throughput, APs' transmit powers are fixed on 2.5 watts with communication range of 260 m for both comparisons. With 0.05 AV/m AV density, the network throughputs achieved by the proposed, the max-utility, and the max-SINR schemes are 0.86 Gbits/s, 0.52 Gbits/s, and 1.12 Gbits/s, respectively. However, both of the max-utility and the max-SINR schemes are ineffective to scenarios with 0.10 AV/m, 0.15 AV/m, and 0.20 AV/m, due to the high inter-cell interferences. From columns 2 to 5 in Table II, the transmit powers of AP 2 and AP 3 for the proposed scheme have been adjusted,

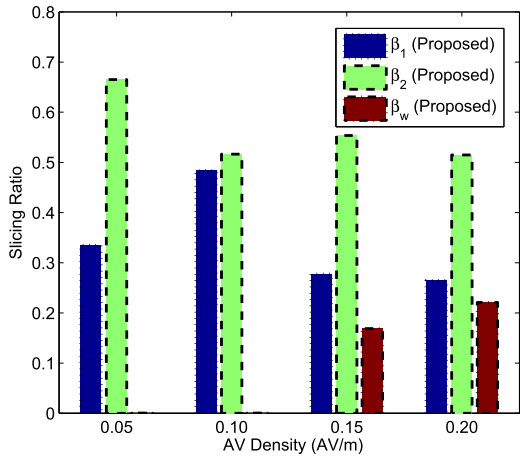

Fig. 6. Spectrum slicing ratios under different AV density for the proposed scheme with $p = 0.8$.

which helps control inter-cell interference for both eNBs and the other two APs' transmissions. Despite the improvement in network throughput, the computational complexity of the proposed scheme is higher than the other two, resulting in more iterations, as shown in columns 6 to 8 of Table II.

In addition to adjusting the transmit powers for the APs, the spectrum slicing ratios among BSs are also adjusted by the proposed scheme, as shown in Fig. 6. With AV density increasing from 0.05 AV/m to 0.20 AV/m, the amount of spectrum resources sliced to Wi-Fi APs, i.e., the spectrum slicing ratio β_w, is increased in the proposed scheme. This is because a large β_w indicates more spectrum resources can be reused among APs and therefore improving the spectrum efficiency.

VI. Conclusions

In this paper, we have proposed a dynamic spectrum management framework to enhance spectrum resource utilization in the MEC-based AVNET with the consideration of cellular and Wi-Fi interworking. Through enabling NFV at the MEC servers, the spectrum resource utilization can be enhanced via dynamically and centrally managing a wide range of spectrum resources and adjusting the transmit power for Wi-Fi APs. To maximize the aggregate network utility and provide QoS-guaranteed downlink transmissions for delay-sensitive and delay-tolerant requests, three optimization problems have been investigated to slice spectrum among BSs fairly, to allocate spectrum among AVs associated with a BS in a QoS-guaranteed way, and to control transmit powers of Wi-Fi APs. In order to solve these three problems, we first use linear programming relaxation and first-order Taylor series approximation to transform them into tractable forms, and then design an ACS algorithm to jointly solve them. Compared with two existing spectrum management schemes, the proposed framework is more robust to AV density changing and provides higher network throughput.

Appendix A
Definitions and Operations

Definition 1 (Second-Order Conditions): Suppose function f is twice differentiable, i.e., it has Hessian or second derivative, $\nabla^2 f$, at each point in its domain, $\mathbf{dom}\, f$. Then f is concave if and only if $\mathbf{dom}\, f$ is a convex set and its second derivative is negative semidefinite for all $y \in \mathbf{dom}\, f$, i.e., $\nabla^2 f \preceq 0$.

To express biconcave set and biconcave function, we define $A \subseteq \mathbb{R}^n$ and $B \subseteq \mathbb{R}^m$ as two non-empty convex sets, and let Y be the Cartesian product of A and B, i.e., $Y \subseteq A \times B$. Define a- and b-sections of Y as $Y_a = \{b \in B : (a, b) \in Y\}$ and $Y_b = \{a \in A : (a, b) \in Y\}$.

Definition 2 (Biconcave Set): Set $Y \subseteq A \times B$ is called as a biconcave set on $A \times B$, if Y_a is convex for every $a \in A$ and Y_b is convex for every $b \in B$.

Definition 3 (Biconcave Function): Define function $f: Y \to \mathbb{R}$ on a biconvex set $Y \subseteq A \times B$. Then function $f: Y \to \mathbb{R}$ is called a biconcave function on Y, if $f_a(b) = f(a, b) : Y_a \to \mathbb{R}$ is a concave function on Y_a for every given $a \in A$, and $f_b(a) = f(a, b) : Y_b \to \mathbb{R}$ is a concave function on Y_b for every given $b \in B$.

Definition 4 (Biconcave Optimization Problem): An optimization problem with form $\max\{f(a, b) : (a, b) \in Y\}$ is called as a biconcave optimization problem, if the feasible set Y is biconvex on Y_a and Y_b, and the objective function $f(a, b)$ is biconcave on Y.

Operation 1 (Nonnegative Weighted Sums): A nonnegative weighted sum of concave functions is concave.

Operation 2 (Composition With an Affine Mapping): Let function $\hbar : \mathbb{R}^n \to \mathbb{R}$, $E \in \mathbb{R}^{n \times m}$, and $e \in \mathbb{R}^n$. Define function $\ell : \mathbb{R}^m \to \mathbb{R}$ by $\ell(y) = \hbar(Ey + e)$ with $\mathbf{dom}\ \ell = \{y | Ey + e \in \mathbf{dom}\ \hbar\}$. Then function ℓ is concave if $\hbar$ is concave.

Appendix B
Proof of Proposition 1

Proof: For problem (P1′), constraint (13a) indicates that $\{\beta_1, \beta_2, \beta_w\}$ is a closed set, i.e., the problem domain is a convex set, and the objective function of (P1′) is the summation of AVs' logarithmic utilities, where the logarithmic function is a concave function due to the non-positive second derivative. Moreover, for an AV associated to a BS, the utility is logarithm of the achievable transmission rate, and the corresponding achievable transmission rate is an affine function of β_1, β_2, or β_w. Thus, based on the above two operations, we can conclude that the objective function of problem (P1′) is a concave function on the three optimal variables β_1, β_2, and β_w. Furthermore, constraint (8a) can be rewritten into inequality concave constraints, such as $\beta_1 \in [0, 1]$ can be as $-\beta_1 \leq 0$ and $\beta_1 \leq 1$, and constraint (8b) is an equality affine function. Therefore, problem (P1′) is a concave optimization problem. □

Appendix C
Proof of Proposition 2

Proof: Constraints (14a)-(14f) of problem (P2′) indicate that $\{\widetilde{\mathbf{X}}, \widetilde{\mathbf{X}}'\}$ and $\{\mathbf{R}, \mathbf{R}'\}$ are convex sets, and Cartesian product is an operation that preserves convexity of convex sets [33]. Thus, the domain of (P2′)', $\{\widetilde{\mathbf{X}}, \widetilde{\mathbf{X}}'\} \times \{\mathbf{R}, \mathbf{R}'\}$, is a convex set. Moreover, as stated before, the objective function of (P2′) is the summation of AVs' achievable transmission rates from

the associated BSs, where the transmission rate achieved by an AV k is an affine function on elements of $\{\mathbf{R}, \mathbf{R}'\}$ for a given association pattern and is an affine function on the association pattern variable for a given resource allocation. Considering the affine function is both concave and convex, it can prove that the objective function of problem (P2′) is a biconcave function on variable set $\{\widetilde{\mathbf{X}}, \widetilde{\mathbf{X}}'\} \times \{\mathbf{R}, \mathbf{R}'\}$. Moreover, constraints (14g) and (14h) are equality affine on $\{\widetilde{\mathbf{X}}, \widetilde{\mathbf{X}}'\}$, constraints (14a)-(14d) are equality biaffine on $\{\widetilde{\mathbf{X}}, \widetilde{\mathbf{X}}'\} \times \{\mathbf{R}, \mathbf{R}'\}$, constraints (14e)-(14f) are respectively inequality affine on $\{\widetilde{\mathbf{X}}, \widetilde{\mathbf{X}}'\}$ and $\{\widetilde{\mathbf{R}}, \widetilde{\mathbf{R}}'\}$, and constraints (14i)-(14p) are inequality biaffine on $\{\widetilde{\mathbf{X}}, \widetilde{\mathbf{X}}'\} \times \{\mathbf{R}, \mathbf{R}'\}$. Thus, we can conclude that (P2′) is a biconcave optimization problem. □

REFERENCES

[1] R. Hussain and S. Zeadally, "Autonomous cars: Research results, issues, and future challenges," *IEEE Commun. Surveys Tuts.*, vol. 21, no. 2, pp. 1275–1313, 2nd Quart., 2019.

[2] L. Li, K. Ota, and M. Dong, "Humanlike driving: Empirical decision-making system for autonomous vehicles," *IEEE Trans. Veh. Technol.*, vol. 67, no. 8, pp. 6814–6823, Aug. 2018.

[3] Z. Su, Y. Hui, and T. H. Luan, "Distributed task allocation to enable collaborative autonomous driving with network softwarization," *IEEE J. Sel. Areas Commun.*, vol. 36, no. 10, pp. 2175–2189, Oct. 2018.

[4] Y. Li, C. Tang, K. Li, X. He, S. Peeta, and Y. Wang, "Consensus-based cooperative control for multi-platoon under the connected vehicles environment," *IEEE Trans. Intell. Transp. Syst.*, vol. 20, no. 6, pp. 2220–2229, Jun. 2018.

[5] H. Peng *et al.*, "Performance analysis of IEEE 802.11p DCF for multiplatooning communications with autonomous vehicles," *IEEE Trans. Veh. Technol.*, vol. 66, no. 3, pp. 2485–2498, Mar. 2017.

[6] H. Peng *et al.*, "Resource allocation for D2D-enabled inter-vehicle communications in multiplatoons," in *Proc. IEEE ICC*, Paris, France, May 2017, pp. 1–6.

[7] H. Peng *et al.*, "Resource allocation for cellular-based inter-vehicle communications in autonomous multiplatoons," *IEEE Trans. Veh. Technol.*, vol. 66, no. 12, pp. 11249–11263, Dec. 2017.

[8] H. Peng, L. Liang, X. Shen, and G. Y. Li, "Vehicular communications: A network layer perspective," *IEEE Trans. Veh. Technol.*, vol. 68, no. 2, pp. 1064–1078, Feb. 2019.

[9] S. Sabău, C. Oară, S. Warnick, and A. Jadbabaie, "Optimal distributed control for platooning via sparse coprime factorizations," *IEEE Trans. Autom. Control*, vol. 62, no. 1, pp. 305–320, Jan. 2017.

[10] H. A. Omar, W. Zhuang, A. Abdrabou, and L. Li, "Performance evaluation of VeMAC supporting safety applications in vehicular networks," *IEEE Trans. Emerg. Topics Comput.*, vol. 1, no. 1, pp. 69–83, Jun. 2013.

[11] X. Cheng, R. Zhang, and L. Yang, *5G-Enabled Vehicular Communications and Networking*. Cham, Switzerland: Springer, 2019.

[12] R. Du, C. Chen, B. Yang, N. Lu, X. Guan, and X. Shen, "Effective urban traffic monitoring by vehicular sensor networks," *IEEE Trans. Veh. Technol.*, vol. 64, no. 1, pp. 273–286, Jan. 2015.

[13] Y. Zhang, H. Zhang, K. Long, Q. Zheng, and X. Xie, "Software-defined and fog-computing-based next generation vehicular networks," *IEEE Commun. Mag.*, vol. 56, no. 9, pp. 34–41, Sep. 2018.

[14] Q. Yuan, H. Zhou, J. Li, Z. Liu, F. Yang, and X. Shen, "Toward efficient content delivery for automated driving services: An edge computing solution," *IEEE Netw.*, vol. 32, no. 1, pp. 80–86, Jan./Feb. 2018.

[15] Y. Hui, Z. Su, T. H. Luan, and J. Cai, "Content in motion: An edge computing based relay scheme for content dissemination in urban vehicular networks," *IEEE Trans. Intell. Transp. Syst.*, to be published.

[16] X. Hou, Y. Li, M. Chen, D. Wu, D. Jin, and S. Chen, "Vehicular fog computing: A viewpoint of vehicles as the infrastructures," *IEEE Trans. Veh. Technol.*, vol. 65, no. 6, pp. 3860–3873, Jun. 2016.

[17] J. Feng, Z. Liu, C. Wu, and Y. Ji, "AVE: Autonomous vehicular edge computing framework with ACO-based scheduling," *IEEE Trans. Veh. Technol.*, vol. 66, no. 12, pp. 10660–10675, Dec. 2017.

[18] K. Abboud, H. A. Omar, and W. Zhuang, "Interworking of DSRC and cellular network technologies for V2X communications: A survey," *IEEE Trans. Veh. Technol.*, vol. 65, no. 12, pp. 9457–9470, Dec. 2016.

[19] European Telecommunications Standards Institute. (Sep. 2018). *ETSI GR MEC 022 V2.1.1 Multi-Access Edge Computing (MEC); Study on MEC Support for V2X Use Cases*. [Online]. Available: https://www.etsi.org/deliver/etsi_gr/MEC/001_099/022/02.01.01_60/gr_MEC022v020101p.pdf

[20] Q. Hu, C. Wu, X. Zhao, X. Chen, Y. Ji, and T. Yoshinaga, "Vehicular multi-access edge computing with licensed sub-6 GHz, IEEE 802.11p and mmWave," *IEEE Access*, vol. 6, pp. 1995–2004, 2017.

[21] H. Peng, Q. Ye, and X. Shen, "SDN-based resource management for autonomous vehicular networks: A multi-access edge computing approach," *IEEE Wireless Commun. Mag.*, to be published.

[22] Z. Su, Y. Wang, Q. Xu, M. Fei, Y.-C. Tian, and N. Zhang, "A secure charging scheme for electric vehicles with smart communities in energy blockchain," *IEEE Internet Things J.*, to be published.

[23] W. Quan, K. Wang, Y. Liu, N. Cheng, H. Zhang, and X. Shen, "Software-defined collaborative offloading for heterogeneous vehicular networks," *Wireless Commun. Mobile Comput.*, vol. 2018, pp. 1–9, Apr. 2018.

[24] J. G. Herrera and J. F. Botero, "Resource allocation in NFV: A comprehensive survey," *IEEE Trans. Netw. Service Manage.*, vol. 13, no. 3, pp. 518–532, Sep. 2016.

[25] G. Luo, J. Li, L. Zhang, Q. Yuan, Z. Liu, and F. Yang, "SDNMAC: A software-defined network inspired MAC protocol for cooperative safety in VANETs," *IEEE Trans. Intell. Transp. Syst.*, vol. 19, no. 6, pp. 2011–2024, Jun. 2018.

[26] G. Secinti, B. Canberk, T. Q. Duong, and L. Shu, "Software defined architecture for VANET: A testbed implementation with wireless access management," *IEEE Commun. Mag.*, vol. 55, no. 7, pp. 135–141, Jul. 2017.

[27] L. Liang, H. Peng, G. Y. Li, and X. Shen, "Vehicular communications: A physical layer perspective," *IEEE Trans. Veh. Technol.*, vol. 66, no. 12, pp. 10647–10659, Dec. 2017.

[28] X. Cheng, L. Yang, and X. Shen, "D2D for intelligent transportation systems: A feasibility study," *IEEE Trans. Intell. Trans. Syst.*, vol. 16, no. 4, pp. 1784–1793, Jan. 2015.

[29] Y. Hui, Z. Su, T. H. Luan, and J. Cai, "A game theoretic scheme for optimal access control in heterogeneous vehicular networks," *IEEE Trans. Intell. Transp. Syst.*, to be published.

[30] Q. Ye, W. Zhuang, S. Zhang, A-L. Jin, X. Shen, and X. Li, "Dynamic radio resource slicing for a two-tier heterogeneous wireless network," *IEEE Trans. Veh. Technol.*, vol. 67, no. 10, pp. 9896–9910, Oct. 2018.

[31] S. K. Jayaweera, G. Vazquez-Vilar, and C. Mosquera, "Dynamic spectrum leasing: A new paradigm for spectrum sharing in cognitive radio networks," *IEEE Trans. Veh. Technol.*, vol. 59, no. 5, pp. 2328–2339, Jun. 2010.

[32] Q. Ye, B. Rong, Y. Chen, M. Al-Shalash, C. Caramanis, and J. G. Andrews, "User association for load balancing in heterogeneous cellular networks," *IEEE Trans. Wireless Commun.*, vol. 12, no. 6, pp. 2706–2716, Jun. 2013.

[33] S. Boyd and L. Vandenberghe, *Convex Optimization*. Cambridge, U.K.: Cambridge Univ. Press, 2004.

[34] J. Gorski, F. Pfeuffer, and K. Klamroth, "Biconvex sets and optimization with biconvex functions: A survey and extensions," *Math. Methods Oper. Res.*, vol. 66, no. 3, pp. 373–407, Dec. 2007.

[35] C. Guo *et al.*, "A fast-converging iterative method based on weighted feedback for multi-distance phase retrieval," *Sci. Rep.*, vol. 8, Apr. 2018, Art. no. 6436.

[36] M. A. Lema *et al.*, "Business case and technology analysis for 5g low latency applications," *IEEE Access*, vol. 5, pp. 5917–5935, 2017.

Haixia Peng (S'15) received the M.S. and Ph.D. degrees in electronics and communication engineering and computer science from Northeastern University, Shenyang, China, in 2013 and 2017, respectively. She is currently pursuing the Ph.D. degree with the Department of Electrical and Computer Engineering, University of Waterloo, Canada. Her current research interests focus on the autonomous vehicular network, resource management, and reinforcement learning. She has served as a TPC member for the IEEE VTC-fall 2016 and 2017, the IEEE ICCEREC 2018, the IEEE Globecom 2016, 2017, 2018, and 2019, and the IEEE ICC 2017, 2018, and 2019 conferences.

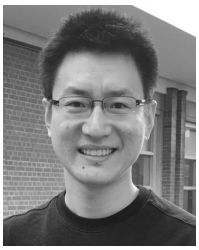

Qiang Ye (S'16–M'17) received the Ph.D. degree in electrical and computer engineering from the University of Waterloo, Waterloo, ON, Canada, in 2016. He is currently a Research Associate with the Department of Electrical and Computer Engineering, University of Waterloo, where he was a Post-Doctoral Fellow, from 2016 to 2018. His current research interests include AI and machine learning for future networking, the IoT, SDN and NFV, network slicing for 5G networks, VNF chain embedding, and end-to-end performance analysis.

Xuemin (Sherman) Shen (M'97–SM'02–F'09) received the Ph.D. degree in electrical engineering from Rutgers University, New Brunswick, NJ, USA, in 1990.

He is currently a University Professor with the Department of Electrical and Computer Engineering, University of Waterloo, Waterloo, ON, Canada. His research interests focus on resource management in interconnected wireless/wired networks, wireless network security, social networks, smart grid and vehicular ad hoc, and sensor networks. He is a registered Professional Engineer of Ontario, Canada, an Engineering Institute of Canada Fellow, a Canadian Academy of Engineering Fellow, a Royal Society of Canada Fellow, and a Distinguished Lecturer of the IEEE Vehicular Technology Society and Communications Society. He received the R.A. Fessenden Award from the IEEE, Canada, in 2019; the James Evans Avant Garde Award from the IEEE Vehicular Technology Society in 2018; the Joseph LoCicero Award and the Education Award from the IEEE Communications Society, in 2015 and 2017, respectively. He has also received the Excellent Graduate Supervision Award in 2006, and the Outstanding Performance Award five times from the University of Waterloo and the Premier's Research Excellence Award (PREA) from the Province of Ontario, Canada, in 2003. He served as the Technical Program Committee Chair/Co-Chair for the IEEE Globecom'16, the IEEE Infocom'14, the IEEE VTC'10 Fall, the IEEE Globecom'07, the Symposia Chair for the IEEE ICC'10, the Tutorial Chair for the IEEE VTC'11 Spring, the Chair for the IEEE Communications Society Technical Committee on Wireless Communications, and P2P Communications and Networking. He is the Editor-in-Chief of the IEEE INTERNET OF THINGS JOURNAL and the Vice President on Publications of the IEEE Communications Society.